Revisiting the Orbital Energy Dependent Regularization of Orbital Optimized Second Order Møller-Plesset Theory

Adam Rettig[#],[†,‡] James Shee[#],[†] Joonho Lee,[¶] and Martin Head-Gordon[*,†,‡]

†*Department of Chemistry, University of California, Berkeley, California 94720, USA*

‡*Chemical Sciences Division, Lawrence Berkeley National Laboratory, Berkeley, California 94720, USA*

¶*Department of Chemistry, Columbia University, New York, New York 10027, USA*

E-mail: mhg@cchem.berkeley.edu

[#] These authors made equal contributions

Abstract

Optimizing orbitals in the presence of electron correlation, as in orbital optimized second-order Møller-Plesset perturbation theory (OOMP2), can remove artifacts associated with mean-field orbitals such as spin contamination and artificial symmetry-breaking. However, OOMP2 is known to suffer from divergent correlation energies in regimes of small orbital energy gaps. To address this issue, several approaches to amplitude regularization have been explored, with those featuring energy-gap dependent regularizers appearing to be most transferable and physically justifiable. For instance, κ-OOMP2 was shown to address the energy divergence issue in, e.g., bond-breaking

processes while offering a significant improvement in accuracy for the W4-11 thermochemistry dataset, and a parameter of κ=1.45 was recommended. A more recent investigation of regularized MP2 with Hartree-Fock orbitals revealed that stronger regularization (i.e. smaller values of κ) than what had previously been recommended for κ-OOMP2 may offer huge improvements in certain cases such as noncovalent interactions while retaining a high level of accuracy for main-group thermochemistry datasets. In this study we investigate the transferability of those findings to κ-OOMP2 and assess the implications of stronger regularization on the ability of κ-OOMP2 to diagnose strong static correlation. We found similar results using κ-OOMP2 for several main-group thermochemistry, barrier height, and noncovalent interaction datasets including both closed shell and open shell species. However, stronger regularization yielded substantially higher accuracy for open-shell transition metal thermochemistry, and is necessary to provide qualitatively correct spin symmetry breaking behavior for several large and electrochemically-relevant transition metal systems. We therefore find a single κ value insufficient to treat all systems using κ-OOMP2.

1 Introduction

Møller-Plesset perturbation theory to second order (MP2) is among the simplest and most widely used correlated wavefunction methods.[1] This is largely a result of its pair-wise additive description of electron correlations at low computation cost, scaling as O(N^5) with system size. The correlation energy is shown in Eq. 1:

$$E_{corr}^{MP2} = -\frac{1}{4}\sum_{ijab}\frac{|\langle ij||ab\rangle|^2}{\Delta_{ij}^{ab}} = \frac{1}{4}\sum_{ijab} t_{ij}^{ab}\langle ij||ab\rangle \tag{1}$$

where i, j and a, b indices represent occupied and virtual molecular orbitals, $\langle ij||ab\rangle$ are antisymmetrized two-electron integrals, and $\Delta_{ij}^{ab} = \epsilon_a + \epsilon_b - \epsilon_i - \epsilon_j$ (ϵ are mean-field orbital

energies). Even such a simplistic treatment of the correlation offers significant improvement over Hartree-Fock (HF), yielding better reaction energies,[2] nonbonded interaction energies,[3] geometries, and properties.[4,5] In addition, MP2 has been incorporated into double hybrid density functional theory (DFT), creating some of the most accurate density functionals currently available.[6–8] In cases where DFT exhibits catastrophic failure due to self-interaction error, MP2 offers a low-cost alternative.[9,10]

Despite MP2's widespread success, it suffers from several shortcomings due to failures of Hartree-Fock (HF) theory as well as shortcomings of low order perturbation theory. MP2, along with other so-called single-reference wavefunction methods, is based upon a single Slater determinant reference and therefore cannot describe strongly correlated electronic systems (in which the wavefunction contains multiple configurations with significant weight). Furthermore, the reference HF state is known to artificially break spin symmetry even in cases which are well-known to be closed-shell and thus single-reference.[11,12] Subsequent perturbation theory (at second order and beyond) based on a spin-contaminated reference determinant can lead to catastrophic energies, geometries, and properties for MP2.[13–16] This shortcoming can be partially ameliorated by strictly enforcing spin symmetry of the reference through use of restricted orbitals, although this leads to qualitative breakdowns of MP2 in cases where the breaking of spin-symmetry is essential such as bond breaking. Finally, MP2 fails in cases where higher order correlation effects are large, and in such cases tends to overestimate the correlation energy, given in equation 1. This is a result of the overestimation of the first order wavefunction amplitudes t_{ij}^{ab} compared to those from infinite-order theories such as coupled cluster with singles and doubles (CCSD), which can arise from either large matrix elements, $\langle \phi_{ij}^{ab} | V | \phi_0 \rangle$, or small orbital energy gaps, Δ_{ij}^{ab}. In this paper we focus on a semi-empirical, but physically motivated, approach to addressing both (1) frequent artificial symmetry breaking of the HF reference and (2) missing correlation effects beyond second order.

The first class of problems arising from artificial symmetry breaking can be fixed via use of alternative orbitals. One interesting choice of non-HF orbitals are those from Kohn-Sham DFT. This route is taken in most double hybrid functionals, although DFT orbitals have additionally been shown to improve the accuracy of higher order wavefunction theories as well.[17,18] The use of DFT orbitals, however, can introduce delocalization error, eliminating one useful feature of MP2. Improved orbitals can also be obtained from within the realm of wavefunction theory by optimizing the orbitals with respect to a Lagrangian associated with the MP2 energy, known as orbital optimized MP2 (OOMP2).[19–25] OOMP2 has been shown to reduce the number of cases exhibiting artificial spin symmetry breaking by approximating Brueckner orbitals.[19,26,27]In systems with large t amplitudes due to already small orbital energy denominators, the use of OOMP2 can push the system toward a zero orbital energy gap in order to decrease the total energy, leading to divergence of the energy as well as the erroneous removal of Coulson-Fischer points.[28] This effect is well visualized in a plot of the largest t amplitudes for several hundred main group molecules as seen in figure 1a; unrestricted OOMP2 (UOOMP2) is seen to yield slightly larger t amplitudes than those obtained with RHF orbitals in nearly all cases, with some species yielding significantly larger t amplitudes. A similar comparison of the HOMO-LUMO gap is seen in figure 1b. In nearly all cases the gap decreases, contributing to the increased t amplitudes; in extreme cases such as bond breaking, this gap can decrease all the way to zero, causing the correlation energy to diverge.

Orbital energy gap dependent regularizers were proposed to correct the divergent behavior of OOMP2, leading to the introduction of κ-OOMP2.[29] In κ-OOMP2, the two electron integrals are damped by a factor depending on the orbital energy difference Δ_{ij}^{ab}, leading to a damping of the t amplitudes as seen in equation 2, as well as an additional damping factor in the energy, as seen in equation 3.

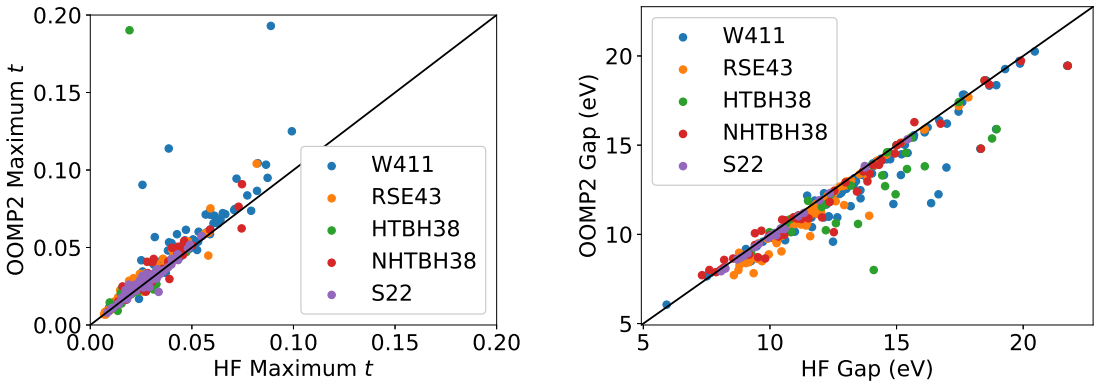

(a) **(b)**

Figure 1: Maximum t amplitudes (a) and orbital energy gaps (b) from UOOMP2 vs. RMP2 (with RHF orbitals) for species involved in the W4-11, RSE43, HTBH38, NHTBH38, and S22 datasets.

$$t_{ij}^{ab(reg)} = t_{ij}^{ab}(1 - e^{-\kappa\Delta_{ij}^{ab}}) \tag{2}$$

$$E_{corr}^{(reg)} = \frac{1}{4}\sum_{ijab} t_{ij}^{ab} \langle ij||ab\rangle \, (1 - e^{-\kappa\Delta_{ij}^{ab}})^2 \tag{3}$$

An important property of this form of regularization is that in the limit of zero-valued orbital energy gaps ($\Delta_{ij}^{ab} \to 0$) there is no contribution to the correlation energy, which removes the divergences seen in unregularized OOMP2. On the other hand, when the orbital energy gap is large ($\Delta_{ij}^{ab} \to \infty$), the t amplitudes will be largely unaffected, preserving the correct behavior of MP2. κ-OOMP2 was seen to restore Coulson-Fischer points in bond breaking applications when using a suitable value of κ.[29] κ-OOMP2 therefore has the potential to remove the artificial spin symmetry breaking seen in HF via orbital optimization with correlation while correctly breaking spin symmetry in cases where it is essential due to regularization. This suggests that predictions of $\langle S^2 \rangle$ from κ-OOMP2 can be an *ab initio* indicator of strong correlation, which may be preferable (at least on grounds of much lower compute costs) to active space methods or analysis of high-scaling coupled cluster

calculations. Indeed, κ-OOMP2 has been used to distinguish between artificial symmetry breaking and essential symmetry breaking in main group chemistry as well as some transition metal (TM) systems.[30–33]

The second class of problems arising from the low order approximation of the correlation energy is somewhat less straightforward to address. Explicit inclusion of higher order correlation as in MP3, CCSD, etc. leads to higher computational cost and is therefore less tractable than MP2 and other related approaches without further approximations. Yet, these higher order methods use the same expression for the correlation energy as MP2 but with different t amplitudes, suggesting that the effect of higher order correlations might be effectively incorporated via tuning the t amplitudes. Scaled MP2 variants such as SCS-MP2[34] and the more efficient SOS-MP2[35] seek to do just that by empirically fitting coefficients to scale the opposite spin and same spin correlation energies, though we note that different optimal coefficients were found for thermochemistry vs non-covalent interactions.[36] The damping of t amplitudes by κ-regularization has been justified previously,[29,37] as an amplitude renormalization due to the effective inclusion of higher order correlations. In this approach, a single parameter gives rise to different scaling coefficients for each t amplitude depending on orbital energy differences, and has been determined through empirical fitting. For example, $\kappa = 1.45$ yields almost a factor of 2 improvement over unregularized OOMP2 for a set of several hundred main group reaction energies (W4-11).[29]

Our group has investigated the use of orbital energy dependent regularizers in standard MP2 on a broad spectrum of systems to quantify the improvement of such a renormalization procedure as well as assess transferability of specific κ values. Assessing the performance of κ-MP2 as a function of κ across main group thermochemistry, barrier heights, noncovalent interactions, and transition metal systems showed a somewhat varied picture. The main group thermochemistry and barrier heights results showed little dependence on the exact κ value; the errors were relatively flat with respect to κ. On the other hand, noncovalent

interactions and transition metal systems showed exceptional improvements when using a significantly stronger regularizer in the range of $\kappa = 0.8 - 1.1$. For these datasets, κ-MP2 yielded up to 3-fold reductions in the root mean squared errors (RMSEs). For this reason, we suggested a κ value of 1.1 for general use.[37]

The present work will conduct an in-depth investigation of κ-OOMP2, using a much more diverse set of datapoints than what was previously considered. We investigate whether κ-OOMP2 also shows a preference for stronger regularization when noncovalent interactions and transition metals are considered. Additionally, we include the extra criterion of symmetry breaking behavior; our suggested value of κ should not be so strong that it reintroduces the artificial symmetry breaking present in HF and it should not be so weak that it does not capture essential symmetry breaking. In this study, we analyze the performance of κ-OOMP2 as a function of κ across thermochemistry, barrier heights, noncovalent interactions, and transition metal chemistry as well as several characteristic essential symmetry breaking problems.

2 Computational Details and Timing

In this work, unrestricted orbitals were used for all datasets. In datasets where results were extrapolated to the complete basis set (CBS) limit, the correlation energy was extrapolated from triple zeta (TZ) and quadruple zeta (QZ) results using the x^{-3} form (where x is 3 for TZ and 4 for QZ)[38] for the correlation energy along with the QZ HF energy of the κ-OOMP2 orbitals. The resolution of the identity (RI) approximation[39] was utilized for all κ-OOMP2 calculations. No frozen core approximation was used.

The W4-11,[40] RSE43,[41,42] HTBH38,[43] and NHTBH38[44] calculations were performed using the aug-cc-pCVTZ/aug-cc-pCVQZ basis sets[45,46] and the aug-cc-pwCVTZ/aug-cc-pwCVQZ RI basis sets.[47] As done in our previous work,[37,48] S22[49] calculations were per-

formed using the aug-cc-pVTZ basis set[45] and corresponding RI basis[50] along with counterpoise correction. For the MCO9 set[37] we again use the def2-QZVPP basis[51,52] with I functions removed, using geometries obtained from ref. 53. We use this basis set for the metallocene calculations as well.

Our investigations of the spin-symmetry breaking behavior as a function of regularization strength do not require large basis sets to adequately describe the electronic structure. Besides, a practical diagnostic for strong static correlation should not require large computational expense. Therefore, for the iron complexes we use the cc-pVDZ[54] (neutral porphyrin, PDI) and def2-SV(P)[52] (charged porphyrin, terpyridine) basis sets, along with the corresponding RI basis sets.[50,55]

All calculations were performed in the Q-Chem package.[56] Relative timings for the κ-OOMP2 implementation included in Q-Chem are given in table 1 for representative systems of varying size (FH, CH_2FCH_2, and benzene-water complex) included in this study. OOMP2 incurs an extra factor of 20 to 30 in the compute time relative to MP2 due to computation of the orbital gradient. Inclusion of the κ regularizer has virtually no effect.

Table 1: Timing (relative to standard RI-MP2) of κ-MP2, OOMP2 (per cycle), and κ-OOMP2 (per cycle) for representative systems of varying size. The number of basis functions (N), occupied orbitals (N_{occ}), virtual orbitals (N_{vir}), and auxiliary basis functions (N_{aux}) is also provided.

System Size	N	N_{occ}	N_{vir}	N_{aux}	MP2	κ-MP2	OOMP2	κ-OOMP2
FH	155	5	150	300	1.00	1.13	5.08	5.08
CH_2FCH_2	511	13	498	986	1.00	1.07	21.62	22.91
benzene-water	1131	26	1105	2194	1.00	1.10	25.19	26.48

3 Results and Discussion

To assess the accuracy and transferability of a single κ value, we tested κ-OOMP2 across a broad distribution of datasets including thermochemistry, barrier heights, and noncovalent interactions spanning both main group chemistry and transition metal chemistry. Addition-

ally, we assessed the utility of each κ value at distinguishing between artificial and essential symmetry breaking via several large transition metal compounds with various types of symmetry breaking behavior.

3.1 Thermochemistry, Barrier Heights, and Noncovalent Interactions

3.1.1 Main Group

The non-MR portion of the W4-11 dataset consists of 83 bond dissociation energies (BDE99), 505 heavy atom transfer reaction energies (HAT707), 20 isomerization energies (ISOMERIZATION20), 13 nucleophilic substitution reaction energies (SN13), and 124 total atomization energies (TAE140). These reactions are comprised of main group species with large gaps whose behavior is typically well captured by standard quantum chemistry methods. Previously, κ-MP2 showed a preference for moderate regularization, although the suggested κ value of 1.1 did little damage to the overall accuracy of the method.[37]

Table 2: RMSE in kcal/mol of κ-OOMP2 with different values of κ for several datasets comprised of main group species.

κ	**W4-11**	**RSE43**	**HTBH38**	**NHTBH38**	**S22**
0 (HF)	57.89	3.10	14.52	11.60	6.20
0.5	17.80	1.38	9.04	8.95	6.19
0.6	14.23	1.24	7.89	7.93	2.48
0.7	11.58	1.13	6.86	6.95	1.91
0.8	9.70	1.02	5.97	6.04	1.01
0.9	8.46	0.92	5.20	5.22	0.67
1.0	7.73	0.83	4.55	4.50	0.41
1.1	7.40	0.75	4.03	3.89	0.27
1.2	7.34	0.68	3.61	3.40	0.32
1.3	7.45	0.63	3.30	3.02	
1.4	7.65	0.59	3.07	2.76	
1.45	7.77	0.57	2.99	2.68	0.65
1.5	7.90	0.56	2.92	2.61	
∞ **(OOMP2)**	10.72	0.85	3.42	3.90	1.52

κ-OOMP2 RMSEs vs CBS extrapolated CCSD(T) reference values for W4-11, seen in table 2, show very little improvement over previous results using κ-MP2.[37] This is unsurprising as the species contained in the W4-11 dataset are well characterized by R(O)HF orbitals. Interestingly, the optimal κ value of 1.2 is significantly stronger than the 1.5 value seen in κ-MP2. As pointed out previously, orbital optimization increases the magnitude of t amplitudes so it is unsurprising that a stronger regularizer is preferred for κ-OOMP2 relative to κ-MP2. It is also noteworthy that the κ-dependence of the RMSE is relatively weak over a broad range: $\kappa = 1.45$ and 1.0 yield similar performance within about 8% of the optimal value of 1.2. Even a regularizer as strong as 0.8 outperforms unregularized OOMP2.

The RSE43 dataset consists of 43 radical stabilization energies; this dataset is known to favor OOMP2 over unrestricted MP2 due to artificial symmetry breaking in the UHF orbitals, so we expect R(O)HF orbitals to narrow the gap between UOOMP2 and MP2 due to elimination of artificial symmetry breaking. κ-OOMP2 RMSEs vs W1-F12 reference values[42] for RSE43 can be seen in table 2. We see that OOMP2 actually performs worse than previous results using MP2,[37] although with a weak regularizer κ-OOMP2 can yield roughly a 20% reduction in error over κ-MP2 suggesting that this is a case of OOMP2 driving towards artificially large t amplitudes. Due to this, we see that OOMP2 actually improves through use of a regularizer unlike κ-MP2 which performed best with no regularization, at least in the range of κ values studied. The exact location of the minimum on the RMSE vs κ surface is unknown due to the boundaries of our scan, however κ values down to around 1.0 seem viable for this dataset. Going below this will provide worse performance than unregularized OOMP2.

The HTBH38 and NHTBH38 datasets consist of 38 hydrogen transfer and non-hydrogen transfer barrier heights respectively. R(O)HF orbitals should be satisfactory for these species due to absence of artificial spin-symmetry breaking so we expect little improvement over κ-MP2. κ-OOMP2 RMSEs vs CBS extrapolated CCSD(T) reference values can be seen in

table 2. For HTBH38, OOMP2 yields a RMSE of 3.42 kcal/mol compared to 4.69 kcal/mol previously seen in MP2.[37] For NHTBH38 on the other hand, OOMP2 performed worse with an RMSE of 3.90 kcal/mol compared to 2.53 kcal/mol previously seen in MP2. The regularization behavior was also slightly different. While MP2 preferred no regularization within the range of κ values studied, κ-OOMP2 offered moderate improvements of 0.3 kcal/mol and 1.3 kcal/mol over unregularized OOMP2 at $\kappa = 1.5$ with possible greater improvements at larger κ values. We therefore once again see a preference for stronger regularization when using orbital optimization.

S22, a set of 22 noncovalent interaction energies, showed drastic improvement through the use of relatively strong regularization in κ-OOMP2, much like κ-MP2. κ-OOMP2 RMSEs vs CBS extrapolated CCSD(T) reference values are given in table 2. OOMP2 yielded a RMSE of 1.52 kcal/mol which is slightly worse than the 1.27 kcal/mol RMSE previously seen in MP2.[37] Due to the tendency of perturbation theory to overestimate noncovalent interactions,[57] using a regularizer with $\kappa = 1.1$ provides over a factor of 5 improvement over OOMP2, yielding a RMSE of 0.27 kcal/mol! This behavior is nearly identical to that seen previously in κ-MP2, which yielded a RMSE of 0.25 kcal/mol with $\kappa = 1.1$. There is therefore no shift towards stronger regularization for this dataset unlike all previous datasets. This suggests that OOMP2 does not lead to larger t amplitudes than RMP2 for this dataset and therefore does not need stronger regularization than RMP2. Figure 1a shows that this is indeed the case; S22 exhibits nearly identical t amplitudes between RHF and OOMP2 orbitals whereas the other datasets exhibit a much broader spread.

Overall, the results for main group chemistry seem extremely similar to previous results seen for κ-MP2 in that the optimal κ value of 1.1-1.5 is fairly large, i.e. weak regularization is preferred. With the exception of S22, the accuracy of κ-OOMP2 is fairly insensitive to the exact κ value and using any κ value within this range offers comparable results. There were two notable differences to our previous κ-MP2 study. The first is that κ-OOMP2

offered noticeable improvements over κ-MP2 for the RSE43 dataset, showing that κ-OOMP2 provides further utility over κ-MP2 by offering higher quality orbitals than ROHF. The other significant difference is a general trend of κ-OOMP2 preferring stronger regularization than κ-MP2; the optimal κ value decreased for W4-11 and actual minima appeared for RSE43, NHTBH38, and HTBH38 which preferred no regularization for MP2. We attributed this behavior to the tendency of orbital optimization to lower the overall energy by increasing the t amplitudes. Interestingly, we see that the shift in optimal κ value is different for each of the datasets - for W4-11 the optimal κ value shifted by 0.3, while for S22 the optimal κ did not change. We account for this difference by looking at the OOMP2 vs the RMP2 maximum t amplitudes in figure 1a. W411, RSE43, HTBH38, and NHTBH38 all contain species where OOMP2 yields significantly larger t amplitudes than R(O)MP2 and therefore require stronger regularizers. S22 however exhibits nearly identical maximum t amplitudes between R(O)MP2 and OOMP2, suggesting that OOMP2 orbitals are nearly identical to R(O)HF orbitals, mitigating the need for a stronger regularizer.

3.1.2 Transition Metals

The MCO9 dataset consists of nine 3d metal-carbonyl complexes (3-6 coordinate) and quantifies the dissociation energy corresponding to a single carbonyl dissociation. Three complexes have singlet ground-states, while the remaining six involve higher multiplicities. In the same spirit as the RSE43 set, this set is therefore an interesting test of the effect of orbital optimization on systems with unpaired electrons. κ-OOMP2 reaction energies are compared directly against experimental reference values, in the same manner as in Ref. 37.

Results for this dataset can be seen in table 3. Data is not provided for unregularized OOMP2 as the resulting correlation energy diverges for several species in this dataset. We find that for some species κ-OOMP2 diverges with $\kappa > 2.0$. Since the κ regularizer yields zero correlation energy in the limit of zero-valued orbital energy gaps in the denominator,

Table 3: RMSE in kcal/mol of κ-OOMP2 with different values of κ for the MCO9 dataset dissociation energies and metallocene dataset ionization energies.

κ	**MCO9**	**Metallocenes**
0.5	5.37	13.95
0.6	2.98	10.49
0.7	4.72	10.17
0.8	7.95	12.52
0.9	11.28	16.04
1.0	14.51	19.89
1.1	17.62	23.55
1.2	20.58	26.25
1.45	27.28	

the orbital optimization procedure must be promoting very large numerators, which is certainly intriguing; we note that infinitely large numerators are formally impossible so these calculations should eventually converge to some very large energy.

It is clear that this dataset shows results quite different than the previous main group datasets. There is a clear preference for significantly stronger regularization, and the optimal κ value of 0.6 gives a RMSE of 2.98 kcal/mol which is over nine times better than $\kappa = 1.45$! Furthermore, the RMSE as a function of κ is extremely steep; most of the main group datasets were relatively flat and using a κ value within 0.2 of the optimal value did not harm results to a large degree. However in this case, using a κ value of 0.8 increases the RMSE to 7.95 kcal/mol, over a factor of two worse.

Previously, κ-MP2 employing the frozen core approximation was seen to yield a RMSE of 5.48 kcal/mol at $\kappa = 0.9$ for the MCO9 dataset[37] (κ-MP2 calculations with all electrons correlated yield an RMSE of 6.9 kcal/mol). It appears that orbital optimization in the presence of strong regularization offers a significant improvement for these cases, suggesting that R(O)HF orbitals provide an inadequate description of the electronic structure. We additionally see a continuation of the trend towards stronger regularization for optimal performance of κ-OOMP2 relative to κ-MP2. Orbital optimization has shifted the minimum on

the RMSE plot from $\kappa = 0.9$ to $\kappa = 0.6$.

The metallocene dataset consists of 7 adiabatic ionization energies, wherein the neutral species and the cation are allowed to relax to different optimal geometries. For this set, only two of the 14 involved species are singlets, and most of the species are spin-symmetry-broken at the UHF level.[58] RMSE vs. experimental references (taken from Ref. 58) as a function of κ can be seen in table 3. The results for this dataset look quite similar to those for the MCO9 dataset, as might be expected since both involve molecules with relatively strong ligand-field strengths (carbonyl and cyclopentadienl ligands coordinate the metal via σ and π bonding). The notably larger minimum RMSE for the metallocene dataset is likely due to the fact that the average energy difference is 142.3 kcal/mol, vs 20.9 kcal/mol for the MCO9 set. Here again, strong regularization is preferred, with the minimum RMSE for the metallocene dataset occuring at $\kappa = 0.7$ compared to 0.6 for MCO9 (both surfaces are quite steep relative to those found for the main group sets). Unregularized OOMP2 once again diverges but the largest κ value for which we could converge all of the calculations gives an RMSE more than a factor of two worse than the minimum.

The behavior of the transition metal datasets is significantly different than for the main group datasets. We see a drastic difference in the optimal κ value, with a value of 0.6-0.7 being preferred here compared to the value of $\kappa = 1.1$ suggested by our main group chemistry datasets. This suggests a larger degree of missing correlation for these datasets leading to even larger errors in the t amplitudes, requiring a stronger regularizer. Figure 2 shows a plot of the maximum t amplitudes for each molecule in a dataset, averaged over the entire dataset, as a function of κ. As suspected, the MCO9 dataset has much larger t amplitudes than other datasets studied; at $\kappa = 1.2$, the MCO9 dataset has an average maximum t amplitude of nearly 0.05 compared to the 0.03 of W4-11, necessitating a stronger regularizer. When using the optimal $\kappa = 0.6$ regularizer for MCO9, the average maximum t amplitude drops to around 0.03, matching W4-11 with its optimal regularizer.

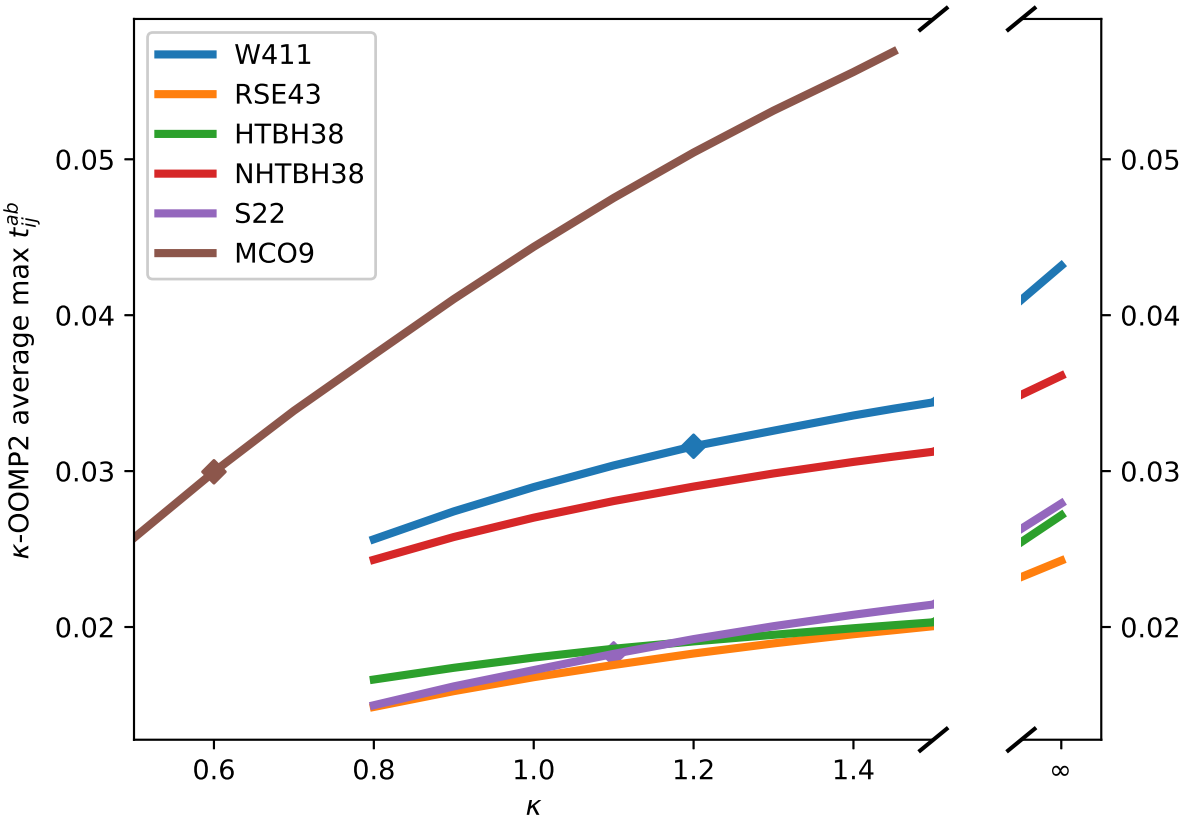

Figure 2: Average of the maximum t amplitude for each species in the dataset as a function of κ. Markers indicate the location of the optimal κ value for each dataset. Dotted line indicates our suggested criteria for adequately damped t amplitudes.

However, it is also evident that the maximum t amplitude does not tell the entire story. The S22 dataset, in comparison to W4-11, prefers a relatively strong regularizer of $\kappa = 1.1$ despite having much smaller average maximum t amplitudes. OOMP2's (and MP2's) overestimation of many noncovalent interaction energies in S22 must therefore arise from slight overestimation of many t amplitudes rather than a vast overestimation of a small subset. Additionally, in many cases the maximum t amplitude corresponds to orbitals localized to one monomer, and therefore any contribution to the interaction energy is largely cancelled out (as the large t amplitude will exist in both the monomer and the dimer) - leading to poor correlation between large t amplitudes and large errors in the interaction energy. For noncovalent interactions, the relevant t amplitudes are therefore only those that involve both monomers (i.e., intermolecular excitations). Thus, while large average maximum t amplitudes can indicate regimes wherein regularization of second order perturbation theory is likely to be beneficial, the damping of a large number of already-small t amplitudes can also have significant effects, and it is possible that the presence of large t amplitudes will not cause large errors in energy differences as their effects will cancel out in, e.g., the calculation of noncovalent interaction energies.

Evidently, the κ regularizer is not capable of treating the wide range of t amplitudes seen across these main group and transition metal datasets in an optimal way with a single choice of the κ parameter. Using a value of $\kappa = 0.7$ to adequately treat the transition metal datasets will lead to very poor results for the main group datasets - the RMSE for W4-11 would increase nearly 50%. However using a value of $\kappa = 1.1$ to adequately treat main group datasets would lead to disastrous results for the transition metal datasets - the RMSE of MCO9 would increase by almost a factor of 6! Compromising between these two cases to a value of $\kappa = 0.9$ leads to intermediate (albeit somewhat unsatisfactory) results in nearly all datasets. We therefore conclude that there is not a value of κ that is optimal for all applications. This is a similar conclusion to what we found for κ-MP2.[37] Additionally,

we propose the maximum t amplitude as a useful metric for ensuring adequate damping of correlation energy contributions, and expect this diagnostic tool to be applicable to κ-MP2 as well. We found that both MCO9 and W4-11 had average maximum t amplitudes of 0.03 at the optimal regularization strength. However, as detailed above, this metric is useful but not comprehensive - the S22 dataset showed that strong regularization can have a substantial effect even if maximum t amplitudes are relatively small.

3.2 Symmetry Breaking

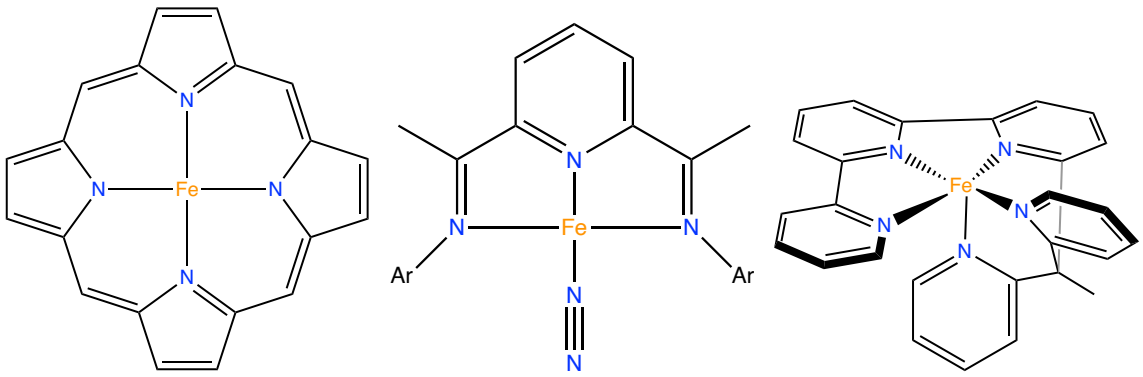

(a) **(b)** **(c)**

Figure 3: Structures of transition metal systems studied (a) FeP (b) FePDI (c) Fe(tpyPY2Me^{2-})

Results across thermochemistry datasets showed very similar, although somewhat exaggerated, regularization preferences relative to κ-MP2. However, κ-OOMP2's utility in distinguishing between artificial and essential spin symmetry breaking should also be considered when determining an optimal κ value. A κ value that is too low will fail to eliminate cases of artificial symmetry breaking, whereas a value that is too high will fail to capture essential symmetry breaking.

Iron porphyrin (FeP), shown in figure 3a, provides a useful test case due to its nontrivial symmetry breaking behavior and plethora of previous single reference[31,59–62] and multireference[63–71] studies as a result of its relevance in several vital biological processes. The ground

state of FeP has previously been characterized as a triplet Fe(II) complex with two unpaired electrons localized on the metal center, which implies this species is well-modeled by a single determinant.[31] However, HF artificially breaks spin symmetry, yielding $\langle S^2 \rangle = 4.91$ with a Mulliken spin on the iron center of 3.87. We therefore expect there is some minimum κ value that ensures spin symmetry will correctly be restored.

κ-OOMP2 with $\kappa = 1.45$ as previously suggested largely corrects the spin symmetry, yielding $\langle S^2 \rangle = 2.11$. However, this solution erroneously shifts some electron spin density off the iron center and onto the porphyrin as seen by the Mulliken spin of 0.96 for this solution, leading to something that looks closer to a species with one unpaired electron on the iron and one on the porphyrin, and an incorrect oxidation state on the iron. Using a stronger regularizer, such as $\kappa = 1.1$, yields a much improved solution with $\langle S^2 \rangle = 2.02$, a Mulliken spin of 2.04, and the correct Fe(II) oxidation state. It therefore seems that there are two κ-OOMP2 solutions for this species - a correct solution with a local triplet on the iron center and an incorrect solution with a local doublet on the iron center. The incorrect solution has a maximum t amplitude of 0.15 - much larger than anything seen in our previous datasets, while the correct solution has a maximum t amplitude of 0.04. Using too weak a regularizer therefore inadequately damps the correlation energy of the incorrect solution, leading to a lower predicted energy than the correct solution.

A plot of the Mulliken spin on the iron center as a function of κ, seen in figure 4a, shows the energy ordering of these solutions switches around $\kappa = 1.2$ with the erroneous solution being the predicted ground state at κ larger than this value and the correct solution being predicted at κ lower than this. This therefore gives an upper bound to the κ value of 1.2 in order to correctly describe the iron porphyrin species. There is also a lower bound at $\kappa = 0.7$ below which artificial symmetry breaking occurs.

A one-electron reduction of FeP yields FeP^- with a doublet ground-state multiplicity. In this configuration, the Fe(II) center is a local triplet coupled anti-ferromagnetically to

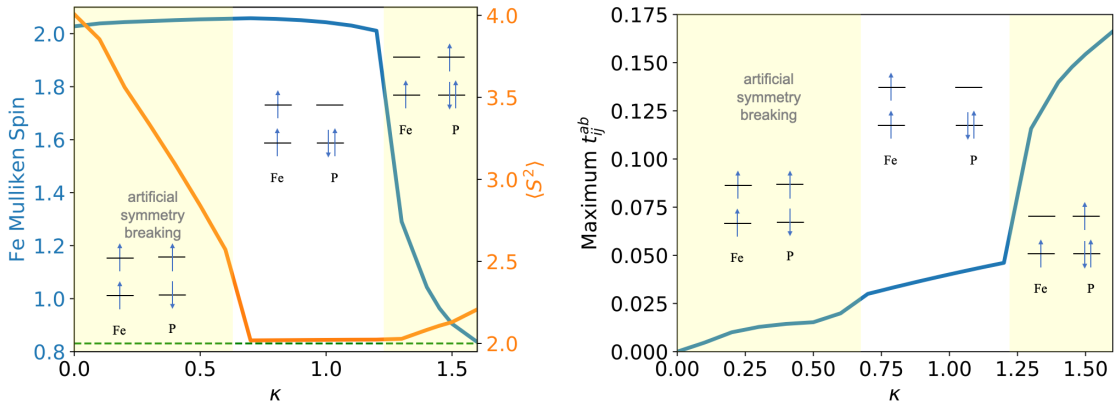

(a) **(b)**

Figure 4: (a) Mulliken spin on the iron and $\langle S^2 \rangle$ of FeP and (b) Maximum t amplitude as a function of κ.

Table 4: Critical κ values for the symmetry breaking systems studied, below which correct symmetry breaking behavior is observed.

System	κ_{crit}
FeP	1.2
FeP^-	1.25
FeP^{2-}	1.2
$Fe(tpyPY2Me^{2-})$	1.05
Fe(PDI)	1.0

a radical in a porphyrin π^* orbital. Unlike the neutral species, strong correlation should therefore be present in the exact wavefunction. In a theory like κ-OOMP2 that lacks *any* treatment of strong correlation, the best description of the open-shell character in FeP^- is via so-called "essential spin symmetry breaking" [30] from an unrestricted variational method, i.e. $\langle S^2 \rangle > 0.75$. In this case we expect to see an upper bound on our κ value, above which spin symmetry is erroneously restored ("artificial symmetry restoration"). This cutoff is found to occur around $\kappa = 1.25$. We note that this artificial symmetry restoration was found in C_{36} in our previous study.[30]

A second reduction to yield FeP^{2-} also happens at the ligand, preserving the Fe(II) oxidation state and local metal triplet. Taken together, the local triplet on the metal is

antiferromagnetically coupled to the ligand-centered local triplet diradical, forming a strongly correlated singlet state. As before, we expect an appropriate parameterization of κ-UOOMP2 to exhibit essential spin-symmetry breaking. As can be seen in figure 5a, one critical κ value is $\kappa = 1.2$, above which artificial spin symmetry restoration leads to physically incorrect closed-shell character. Another critical κ value is found around $\kappa = 0.7$, below which the solution begins artificially spin polarizing once again to converge to the HF solution at $\kappa = 0$. In this regime of artificial symmetry breaking, the local spin density on the iron atom is incorrectly predicted to be 0. For this species we therefore require $0.7 \leq \kappa < 1.2$. Analogous critical κ values are collected in Table 4.

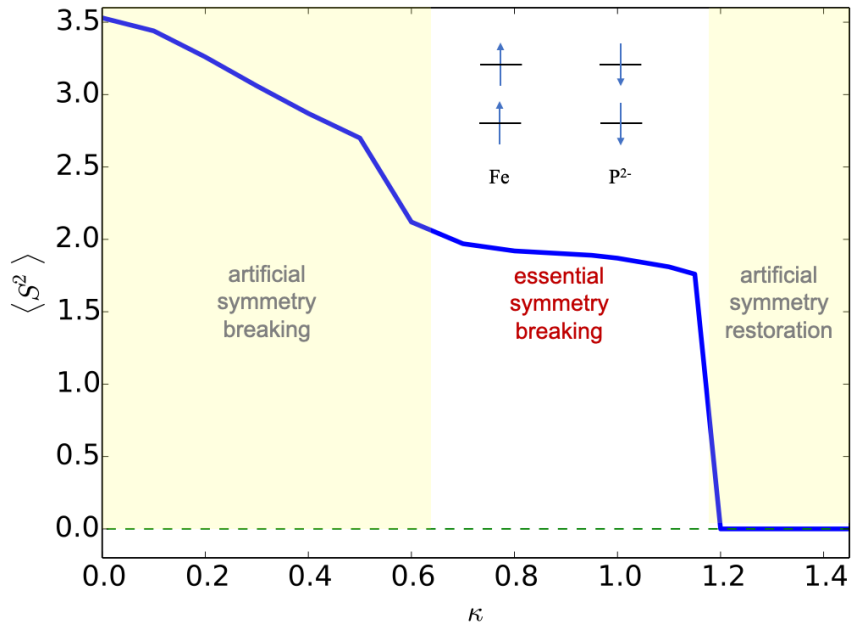

(a)

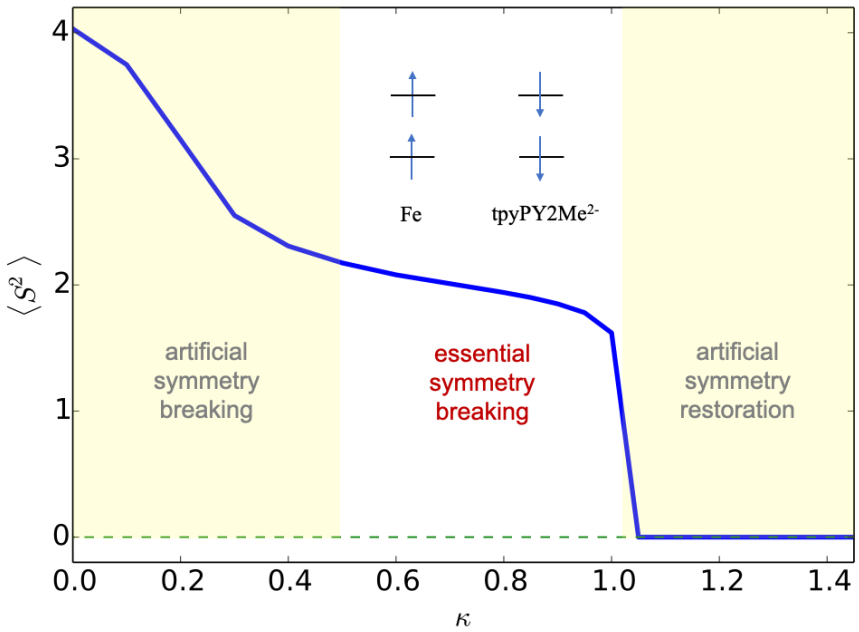

(b)

Figure 5: $\langle S^2 \rangle$ vs. κ for (a) FeP^{2-} and (b) Fe(tpyPY2Me^{2-}). The dotted lines indicate the exact value of S^2 for a singlet. The regime of artificial symmetry restoration corresponds to incorrect closed-shell singlet character. Essential symmetry breaking utilizes contributions from primarily the $m_s = 0$ quintet state to describe the antiferromagnetic coupling between local triplets to form a strongly correlated open-shell singlet state. Artificial symmetry breaking indicates the presence of spurious contributions from even higher spin multiplicities, recovering the UHF state in the limit of $\kappa \to 0$.

Another interesting test case is an Fe complex with a twice-reduced terpyridine-based pentapyridine ligand (tpyPY2Me^{2-}), shown in figure 3c, which has a charge-neutral ground-state exhibiting analogous multi-reference character to FeP^{2-}.[33,72] The physically correct single-reference state should be spin-symmetry broken (i.e. $\langle S^2 \rangle > 0$), again due to metal-ligand anti-ferromagnetic coupling. One critical κ value for this system, seen in figure 5b, is $\kappa_{crit} = 1.0$, necessitating an even stronger regularizer than the iron porphyrin systems to adequately describe the spin symmetry. As before, when $\kappa > 1.0$ a closed shell singlet is incorrectly recovered. The second critical κ occurs at $\kappa_{crit} = 0.5$, below which we see a steep rise in the $\langle S^2 \rangle$ plot to erroneously further break spin symmetry (the local spin density of the iron remains two). For this case we therefore require $0.5 \leq \kappa \leq 1.0$.

Lastly, we consider (PDI)Fe-N_2, where PDI is 2,6-bis[1-(2,6-dimethyphenyl-imino)thyl]pyridine (henceforth referred to simply as Fe(PDI)), as shown in figure 3b. This species was previously shown to have a singlet ground state with a low-lying triplet state. The magnitude of the singlet-triplet (S-T) gap has been somewhat debated as different computational methods yield vastly different results.[73–75] Recent multireference approaches show both of these states are characterized by spin symmetry broken solutions - the singlet having an unpaired electron on the iron center anti-ferromagnetically coupled to one on the PDI and the triplet having three unpaired electrons on the iron center with one anti-ferromagnetically coupled to one on the PDI. We focus on the triplet in this case.

This system looks much like the reduced iron porphyrin species previously mentioned, so it is unsurprising we see very similar behavior. κ-OOMP2 incorrectly restores spin symmetry at $\kappa > 1.0$, predicting a nearly spin pure triplet ($\langle S^2 \rangle$ close to 2) with one unpaired electron on the iron center and one on the PDI. Using a stronger regularizer with $\kappa \leq 1.0$ correctly breaks spin symmetry and yields a Mulliken spin on the iron close to 3 as expected. This system therefore also requires a fairly strong regularizer.

Considering all these systems with nontrivial spin symmetry provides a clear motivation

for strong regularization. In each case, using too weak a regularizer led to qualitatively incorrect solutions due to insufficient damping of erroneous t amplitudes in solutions other than the ground state. To correctly capture even qualitatively correct behavior across all systems considered, we must use a κ value of 1.0 or below, although the exact value required varies system to system. For these cases, we see the erroneous solution present with weak regularizers exhibits extremely large t amplitudes indicating a breakdown of perturbation theory. In most of these cases, the breakdown is so severe that UOOMP2 diverges. It is therefore unsurprising that we need a stronger regularizer.

κ-UOOMP2 in the limit of $\kappa \to 0$ recovers UHF, which predicts $\langle S^2 \rangle$ values of 4.00, 3.24, 3.53, 4.03, and 5.06 for the ground-states of FeP, Fe^{1-}, FeP^{2-}, Fe(tpyPY2Me^{2-}), and Fe(PDI), respectively. In all of these cases, the degree of spin-contamination is higher than what is found with κ-UOOMP2 in κ regimes that recover physical, or "essential" spin symmetry breaking. There is therefore a second critical value of κ at values smaller than the values noted in Table 4, which marks the onset of artificial spin-symmetry breaking. For the systems studied, this second critical κ occurred around 0.5-0.7. We therefore need a κ value between 0.7 and 1.0 to qualitatively capture the symmetry breaking behavior of all the transition metal systems studied.

Of the symmetry breaking systems previously studied with κ-OOMP2, C_{60} is of special note as using a stronger regularizer would result in a broken symmetry solution, indicating a strongly correlated system in contradiction to previous results.[30] However, this system exhibits a maximum t amplitude of 0.014 at $\kappa = 1.45$, suggesting that this is not a qualitative breakdown of perturbation theory and the previous conclusions are valid.

4 Conclusions

While optimizing orbitals in the presence of MP2 correlation (OOMP2) can greatly reduce artifacts of mean-field Hartree-Fock (HF) orbitals, the non-variational nature of the total energy means that regularization of the amplitudes is required. The energy-dependent κ-OOMP2 approach to regularization connects the HF limit (very strong regularization: $\kappa \to 0$) and the OOMP2 limit (very weak regularization: $\kappa \to \infty$). With judicious choice of κ, κ-OOMP2 was shown to offer significant, and sometimes dramatic improvements over OOMP2 (or MP2) across a wide variety of applications, as well as preventing divergence of the correlation energy during orbital optimization. This regularization can be justified as a renormalization of the MP2 amplitudes that mimics to some extent the neglected effects of higher than second order correlation effects. Significant improvement over using just HF orbitals (i.e. κ-OOMP2 vs κ-MP2) was also seen, supporting the importance of orbital optimization, particularly for transition metal and radical systems. Additionally, use of the frozen core approximation could further extend the applicability of κ-OOMP2, allowing its use in even larger systems than studied here.

For main group chemistry, including thermochemistry, barrier heights, and noncovalent interactions, a κ value of 1.1 was seen to be generally satisfactory, although most datasets were not quite so sensitive to the exact value. In nearly all cases, this value offered significant improvement over unregularized OOMP2. However, for predominately open-shell transition metal thermochemistry datasets, where both R(O)HF and UHF orbitals are expected to be inadequate, we find a strong preference for much stronger regularization; κ-OOMP2 performed best with a value of $\kappa = 0.6 - 0.7$. With these much stronger regularizers, κ-OOMP2 showed very significant improvement, especially since unregularized OOMP2 diverges for these species.

While a single value of κ was not seen to yield satisfactory results for all types of datasets

considered, we have also shown that a lot of useful information about the electronic structure of a molecule can be gleaned by scanning the κ parameter. Indeed, we extended our investigation beyond the quantitative prediction of reaction energies by considering the symmetry breaking behavior of κ-OOMP2. Looking at several large transition metal complexes exhibiting both essential and artificial symmetry breaking, we found a preference for stronger regularization, with a value of $\kappa \leq 1.0$ required to yield proper descriptions of all systems included in this study. A lower bound of $\kappa > 0.6$ was also determined, below which the spin symmetry breaking is seen to be artificial.

It therefore seems improper to prescribe a global value of κ for use in every situation. Instead, for systems of particular interest, we suggest scanning over κ and monitoring the maximum t amplitudes for the species considered. This reveals the artifacts such as symmetry-breaking associated with HF orbitals for small κ, and artifacts of OOMP2 such as nonvariational energies and artificial symmetry restoration for large κ. The behavior of κ-OOMP2 in intermediate regimes is then particularly interesting: the presence of essential symmetry breaking is an indicator of the presence of strong correlations in that systems.

For chemical applications, scanning κ is too inconvenient to recommend seriously. Instead we can offer a few conclusions based on the extensive data we have presented here:

1. There is no universally optimum choice of κ for chemical applications. However, in almost all tests reported here, the value of $\kappa = 1.45$ initially recommended by two of us[29] is too weak to be recommended for routine use.

2. The *weakest* regularizer that we can recommend is $\kappa = 1.1$, consistent with the careful optimization that we have performed for κ-MP2 (i.e. without orbital optimization).[37] This seems very effective for most applications to main group chemistry reported here, but is demonstrably too weak for our transition metal tests.

3. The *strongest* regularizer that we can recommend is $\kappa = 0.65$ which appears to be very

effective for tests of transition metal systems, though it is demonstrably too strong for the main group chemistry tests. Therefore a compromise value of $\kappa = 0.9$ can also be supported, although it is not optimal for *either* our main group or transition metal tests.

4. Monitoring the largest t amplitude can be an indicator of the need for stronger regularization, while monitoring measures of artificial symmetry-breaking can be an indicator of the need for weaker regularization.

The inability to recover high accuracy in both limiting situations with a single regularization parameter shows that limitations of OOMP2 cannot be fully overcome by regularization based only on orbital energy denominators. We postulate that a regularizer dependent on the entire t amplitude rather than solely on the energy denominator could prove more transferable. However even there, we expect difficulties arising from cases such as S22 which requires regularization despite small t amplitudes. In designing new t amplitude-based regularizers, care must be taken to ensure properties related to differentiability and orbital invariances to occupied-occupied and virtual-virtual rotations.

This study has implications for several other methods built upon κ-OOMP2. When performing higher order methods, such as MP3 or coupled cluster, using κ-OOMP2 orbitals, a stronger regularizer would likely be preferable to ensure qualitatively correct orbitals as the κ-OOMP2 energy is not used. We also think a regularized orbital optimized double hybrid density functional theory[76] could achieve even higher accuracy than current functionals, as benefits have already been noted for regularized double hybrid DFT.[77] However, we have shown that careful consideration across a broad selection of applications to ensure transferability is necessary for this sort of functional development.

5 Associated Content

Supporting Information: This material is available free of charge at the website http://pubs.acs.org/

- Individual reaction energies for all datasets as a function of κ (XLSX)

Acknowledgements: This work was supported by the Director, Office of Science, Office of Basic Energy Sciences, of the U.S. Department of Energy under Contract No. DE-AC02-05CH11231. This research used resources of the National Energy Research Scientific Computing Center (NERSC), a U.S. Department of Energy Office of Science User Facility located at Lawrence Berkeley National Laboratory. A.R. acknowledges funding from the National Science Foundation under award number DGE 1752814. J.S. acknowledges funding from the National Institute of General Medical Sciences of the National Institutes of Health under award number F32GM142231. We acknowledge additional support from the National Institutes of Health under Grant No. 5U01GM121667. J.L. thanks David Reichman for support.

References

(1) Cremer, D. Moller-Plesset perturbation theory: from small molecule methods to methods for thousands of atoms. *Wiley Interdiscip. Rev.: Comput. Mol. Sci.* **2011**, *1*, 509–530.

(2) Helgaker, T.; Jørgensen, P.; Olsen, J. *Molecular Electronic-Structure Theory*; John Wiley & Sons, 2000.

(3) Goldey, M.; Dutoi, A.; Head-Gordon, M. Attenuated second order Moller-Plesset the-

ory: Assessment and performance in the aug-cc-pVTZ basis. *Phys. Chem. Chem. Phys.* **2013**, *15*, 15869.

(4) Hait, D.; Head-Gordon, M. How accurate is density functional theory at predicting dipole moments? An assessment using a new database of 200 benchmark values. *J. Chem. Theory Comput.* **2018**, *14*, 1969–1981.

(5) Hait, D.; Head-Gordon, M. How accurate are static polarizability predictions from density functional theory? An assessment over 132 species at equilibrium geometry. *Phys. Chem. Chem. Phys.* **2018**, *20*, 19800–19810.

(6) Goerigk, L.; Grimme, S. Double-hybrid density functionals. *Wiley Interdiscip. Rev.: Comput. Mol. Sci.* **2014**, *4*, 576–600.

(7) Mardirossian, N.; Head-Gordon, M. Survival of the most transferable at the top of Jacob's ladder: Defining and testing the ωB97M(2) double hybrid density functional. *J. Chem. Phys.* **2018**, *148*, 241736.

(8) Martin, J. M. L.; Santra, G. Empirical double-hybrid density functional theory: A 'third way' in between WFT and DFT. *Isr. J. Chem.* **2020**, *60*, 787–804.

(9) Zhang, Y.; Yang, W. A challenge for density functionals: Self-interaction error increases for systems with a noninteger number of electrons. *J. Chem. Phys.* **1998**, *109*, 2604–2608.

(10) Mori-Sánchez, P.; Cohen, A. J.; Yang, W. Many-electron self-interaction error in approximate density functionals. *J. Chem. Phys.* **2006**, *125*, 201102.

(11) Davidson, E. R.; Borden, W. T. Symmetry breaking in polyatomic molecules: real and artifactual. *The Journal of Physical Chemistry* **1983**, *87*, 4783–4790.

(12) Paldus, J.; Thiamová, G. Approximate symmetry-breaking in the independent particle model of monocyclic completely conjugated polyenes. *Journal of mathematical chemistry* **2008**, *44*, 88–120.

(13) Farnell, L.; Pople, J. A.; Radom, L. Structural predictions for open-shell systems: a comparative assessment of ab initio procedures. *The Journal of Physical Chemistry* **1983**, *87*, 79–82.

(14) Nobes, R. H.; Pople, J. A.; Radom, L.; Handy, N. C.; Knowles, P. J. Slow convergence of the møller-plesset perturbation series: the dissociation energy of hydrogen cyanide and the electron affinity of the cyano radical. *Chemical physics letters* **1987**, *138*, 481–485.

(15) Gill, P. M.; Pople, J. A.; Radom, L.; Nobes, R. H. Why does unrestricted Mo/ller–Plesset perturbation theory converge so slowly for spin-contaminated wave functions? *The Journal of chemical physics* **1988**, *89*, 7307–7314.

(16) Jensen, F. A remarkable large effect of spin contamination on calculated vibrational frequencies. *Chemical physics letters* **1990**, *169*, 519–528.

(17) Rettig, A.; Hait, D.; Bertels, L. W.; Head-Gordon, M. Third-order Møller–Plesset theory made more useful? The role of density functional theory orbitals. *J. Chem. Theory Comput.* **2020**, *16*, 7473–7489.

(18) Bertels, L. W.; Lee, J.; Head-Gordon, M. Polishing the gold standard: The role of orbital choice in CCSD (T) vibrational frequency prediction. *Journal of chemical theory and computation* **2021**, *17*, 742–755.

(19) Lochan, R. C.; Head-Gordon, M. Orbital-optimized opposite-spin scaled second-order correlation: An economical method to improve the description of open-shell molecules. *J. Chem. Phys.* **2007**, *126*, 164101.

(20) Neese, F.; Schwabe, T.; Kossmann, S.; Schirmer, B.; Grimme, S. Assessment of orbital-optimized, spin-component scaled second-order many-body perturbation theory for thermochemistry and kinetics. *J. Chem. Theory Comput.* **2009**, *5*, 3060–3073.

(21) Bozkaya, U.; Turney, J. M.; Yamaguchi, Y.; Schaefer III, H. F.; Sherrill, C. D. Quadratically convergent algorithm for orbital optimization in the orbital-optimized coupled-cluster doubles method and in orbital-optimized second-order Møller-Plesset perturbation theory. *The Journal of chemical physics* **2011**, *135*, 104103.

(22) Bozkaya, U. Orbital-optimized second-order perturbation theory with density-fitting and Cholesky decomposition approximations: An efficient implementation. *J. Chem. Theory Comput.* **2014**, *10*, 2371–2378.

(23) Bozkaya, U. Analytic energy gradients and spin multiplicities for orbital-optimized second-order perturbation theory with density-fitting approximation: an efficient implementation. *Journal of Chemical Theory and Computation* **2014**, *10*, 4389–4399.

(24) Bozkaya, U.; Sherrill, C. D. Analytic energy gradients for the orbital-optimized second-order Møller–Plesset perturbation theory. *The Journal of Chemical Physics* **2013**, *138*, 184103.

(25) Soydaş, E.; Bozkaya, ğ. Accurate open-shell noncovalent interaction energies from the orbital-optimized Møller–Plesset perturbation theory: Achieving CCSD quality at the MP2 level by orbital optimization. *Journal of Chemical Theory and Computation* **2013**, *9*, 4679–4683.

(26) Dykstra, C. E. An examination of the Brueckner condition for the selection of molecular orbitals in correlated wavefunctions. *Chemical Physics Letters* **1977**, *45*, 466–469.

(27) Handy, N. C.; Pople, J. A.; Head-Gordon, M.; Raghavachari, K.; Trucks, G. W. Size-

consistent Brueckner theory limited to double substitutions. *Chemical physics letters* **1989**, *164*, 185–192.

(28) Sharada, S. M.; Stück, D.; Sundstrom, E. J.; Bell, A. T.; Head-Gordon, M. Wavefunction stability analysis without analytical electronic hessians: Application to orbital-optimized post-Hartree-Fock methods and VV10-containing density functionals. *Mol. Phys.* **2015**, *113*, 1802.

(29) Lee, J.; Head-Gordon, M. Regularized orbital-optimized second-order Møller–Plesset perturbation theory: A reliable fifth-order-scaling electron correlation model with orbital energy dependent regularizers. *J. Chem. Theory Comput.* **2018**, *14*, 5203–5219.

(30) Lee, J.; Head-Gordon, M. Distinguishing artificial and essential symmetry breaking in a single determinant: Approach and application to the C_{60}, C_{36}, and C_{20} fullerenes. *Phys. Chem. Chem. Phys.* **2019**, *21*, 4763–4768.

(31) Lee, J.; Malone, F. D.; Morales, M. A. Utilizing essential symmetry breaking in auxiliary-field quantum Monte Carlo: Application to the spin gaps of the C36 fullerene and an iron porphyrin model complex. *Journal of chemical theory and computation* **2020**, *16*, 3019–3027.

(32) Lee, J.; Head-Gordon, M. Two single-reference approaches to singlet biradicaloid problems: Complex, restricted orbitals and approximate spin-projection combined with regularized orbital-optimized Møller-Plesset perturbation theory. *J. Chem. Phys.* **2019**, *150*, 244106.

(33) Shee, J.; Loipersberger, M.; Hait, D.; Lee, J.; Head-Gordon, M. Revealing the nature of electron correlation in transition metal complexes with symmetry breaking and chemical intuition. *J. Chem. Phys.* **2021**, *154*, 194109.

(34) Grimme, S. Improved second-order Møller–Plesset perturbation theory by separate scaling of parallel-and antiparallel-spin pair correlation energies. *J. Chem. Phys.* **2003**, *118*, 9095–9102.

(35) Jung, Y.; Lochan, R. C.; Dutoi, A. D.; Head-Gordon, M. Scaled opposite-spin second order Møller–Plesset correlation energy: an economical electronic structure method. *J. Chem. Phys.* **2004**, *121*, 9793.

(36) DiStasio, Jr., R. A.; Head-Gordon, M. Optimized spin-component scaled second-order Møller-Plesset perturbation theory for intermolecular interaction energies. *Mol. Phys.* **2007**, *105*, 1073.

(37) Shee, J.; Loipersberger, M.; Rettig, A.; Lee, J.; Head-Gordon, M. Regularized second-order Møller–Plesset theory: A more accurate alternative to conventional MP2 for noncovalent interactions and transition metal thermochemistry for the same computational cost. *The Journal of Physical Chemistry Letters* **2021**, *12*, 12084–12097.

(38) Helgaker, T.; Klopper, W.; Koch, H.; Noga, J. Basis-set convergence of correlated calculations on water. *J. Chem. Phys.* **1997**, *106*, 9639–9646.

(39) Feyereisen, M.; Fitzgerald, G.; Komornicki, A. Use of approximate integrals in ab initio theory. An application in MP2 energy calculations. *Chem. Phys. Lett.* **1993**, *208*, 359–363.

(40) Karton, A.; Daon, S.; Martin, J. M. W4-11: A high-confidence benchmark dataset for computational thermochemistry derived from first-principles W4 data. *Chem. Phys. Lett.* **2011**, *510*, 165–178.

(41) Zipse, H. Radical stability—a theoretical perspective. *Radicals in Synthesis I* **2006**, 163–189.

(42) Goerigk, L.; Hansen, A.; Bauer, C.; Ehrlich, S.; Najibi, A.; Grimme, S. A look at the density functional theory zoo with the advanced GMTKN55 database for general main group thermochemistry, kinetics and noncovalent interactions. *Phys. Chem. Chem. Phys.* **2017**, *19*, 32184–32215.

(43) Zhao, Y.; Lynch, B. J.; Truhlar, D. G. Multi-coefficient extrapolated density functional theory for thermochemistry and thermochemical kinetics. *Physical Chemistry Chemical Physics* **2005**, *7*, 43–52.

(44) Zhao, Y.; González-García, N.; Truhlar, D. G. Benchmark database of barrier heights for heavy atom transfer, nucleophilic substitution, association, and unimolecular reactions and its use to test theoretical methods. *The Journal of Physical Chemistry A* **2005**, *109*, 2012–2018.

(45) Kendall, R. A.; Dunning Jr, T. H.; Harrison, R. J. Electron affinities of the first-row atoms revisited. Systematic basis sets and wave functions. *The Journal of chemical physics* **1992**, *96*, 6796–6806.

(46) Woon, D. E.; Dunning Jr, T. H. Gaussian basis sets for use in correlated molecular calculations. V. Core-valence basis sets for boron through neon. *The Journal of chemical physics* **1995**, *103*, 4572–4585.

(47) Hättig, C. Optimization of auxiliary basis sets for RI-MP2 and RI-CC2 calculations: Core–valence and quintuple-ζ basis sets for H to Ar and QZVPP basis sets for Li to Kr. *Physical Chemistry Chemical Physics* **2005**, *7*, 59–66.

(48) Loipersberger, M.; Bertels, L. W.; Lee, J.; Head-Gordon, M. Exploring the Limits of Second-and Third-Order Møller–Plesset Perturbation Theories for Noncovalent Interactions: Revisiting MP2. 5 and Assessing the Importance of Regularization and Reference Orbitals. *J. Chem. Theory Comput.* **2021**,

(49) Jurecka, P.; Sponer, J.; Cerny, J.; Hobza, P. *Phys. Chem. Chem. Phys.* **2006**, *8*, 1985.

(50) Weigend, F.; Köhn, A.; Hättig, C. Efficient use of the correlation consistent basis sets in resolution of the identity MP2 calculations. *The Journal of chemical physics* **2002**, *116*, 3175–3183.

(51) Weigend, F.; Furche, F.; Ahlrichs, R. Gaussian basis sets of quadruple zeta valence quality for atoms H–Kr. *The Journal of chemical physics* **2003**, *119*, 12753–12762.

(52) Weigend, F.; Ahlrichs, R. Balanced basis sets of split valence, triple zeta valence and quadruple zeta valence quality for H to Rn: Design and assessment of accuracy. *Physical Chemistry Chemical Physics* **2005**, *7*, 3297–3305.

(53) Rudshteyn, B.; Coskun, D.; Weber, J. L.; Arthur, E. J.; Zhang, S.; Reichman, D. R.; Friesner, R. A.; Shee, J. Predicting ligand-dissociation energies of 3d coordination complexes with auxiliary-field quantum Monte Carlo. *J. Chem. Theory Comput.* **2020**, *16*, 3041–3054.

(54) Dunning Jr, T. H. Gaussian basis sets for use in correlated molecular calculations. I. The atoms boron through neon and hydrogen. *The Journal of chemical physics* **1989**, *90*, 1007–1023.

(55) Weigend, F.; Häser, M.; Patzelt, H.; Ahlrichs, R. RI-MP2: optimized auxiliary basis sets and demonstration of efficiency. *Chemical physics letters* **1998**, *294*, 143–152.

(56) Epifanovsky, E.; Gilbert, A. T.; Feng, X.; Lee, J.; Mao, Y.; Mardirossian, N.; Pokhilko, P.; White, A. F.; Coons, M. P.; Dempwolff, A. L., et al. Software for the frontiers of quantum chemistry: An overview of developments in the Q-Chem 5 package. *J. Chem. Phys.* **2021**, *155*, 084801.

(57) Nguyen, B. D.; Chen, G. P.; Agee, M. M.; Burow, A. M.; Tang, M. P.; Furche, F. Divergence of many-body perturbation theory for noncovalent interactions of large molecules. *J. Chem. Theory Comput.* **2020**, *16*, 2258–2273.

(58) Rudshteyn, B.; Weber, J. L.; Coskun, D.; Devlaminck, P. A.; Zhang, S.; Reichman, D. R.; Shee, J.; Friesner, R. A. Calculation of Metallocene Ionization Potentials via Auxiliary Field Quantum Monte Carlo: Toward Benchmark Quantum Chemistry for Transition Metals. *Journal of Chemical Theory and Computation* **2022**, *18*, 2845–2862.

(59) Rovira, C.; Kunc, K.; Hutter, J.; Ballone, P.; Parrinello, M. Equilibrium geometries and electronic structure of iron- porphyrin complexes: A density functional study. *The Journal of Physical Chemistry A* **1997**, *101*, 8914–8925.

(60) Groenhof, A. R.; Swart, M.; Ehlers, A. W.; Lammertsma, K. Electronic ground states of iron porphyrin and of the first species in the catalytic reaction cycle of cytochrome P450s. *The Journal of Physical Chemistry A* **2005**, *109*, 3411–3417.

(61) Matsuzawa, N.; Ata, M.; Dixon, D. A. Density functional theory prediction of the second-order hyperpolarizability of metalloporphines. *The Journal of Physical Chemistry* **1995**, *99*, 7698–7706.

(62) Radon, M. Spin-state energetics of heme-related models from DFT and coupled cluster calculations. *Journal of Chemical Theory and Computation* **2014**, *10*, 2306–2321.

(63) Radon, M.; Pierloot, K. Binding of CO, NO, and O2 to heme by density functional and multireference ab initio calculations. *The Journal of Physical Chemistry A* **2008**, *112*, 11824–11832.

(64) Choe, Y.-K.; Nakajima, T.; Hirao, K.; Lindh, R. Theoretical study of the electronic

ground state of iron (II) porphine. II. *The Journal of chemical physics* **1999**, *111*, 3837–3845.

(65) Pierloot, K. The CASPT2 method in inorganic electronic spectroscopy: from ionic transition metal to covalent actinide complexes. *Molecular physics* **2003**, *101*, 2083–2094.

(66) Phung, Q. M.; Feldt, M.; Harvey, J. N.; Pierloot, K. Toward highly accurate spin state energetics in first-row transition metal complexes: a combined CASPT2/CC approach. *Journal of chemical theory and computation* **2018**, *14*, 2446–2455.

(67) Vancoillie, S.; Zhao, H.; Tran, V. T.; Hendrickx, M. F.; Pierloot, K. Multiconfigurational second-order perturbation theory restricted active space (RASPT2) studies on mononuclear first-row transition-metal systems. *Journal of Chemical Theory and Computation* **2011**, *7*, 3961–3977.

(68) Olivares-Amaya, R.; Hu, W.; Nakatani, N.; Sharma, S.; Yang, J.; Chan, G. K.-L. The ab-initio density matrix renormalization group in practice. *The Journal of chemical physics* **2015**, *142*, 034102.

(69) Phung, Q. M.; Wouters, S.; Pierloot, K. Cumulant approximated second-order perturbation theory based on the density matrix renormalization group for transition metal complexes: A benchmark study. *Journal of chemical theory and computation* **2016**, *12*, 4352–4361.

(70) Li Manni, G.; Alavi, A. Understanding the mechanism stabilizing intermediate spin states in Fe (II)-porphyrin. *The Journal of Physical Chemistry A* **2018**, *122*, 4935–4947.

(71) Zhou, C.; Gagliardi, L.; Truhlar, D. G. Multiconfiguration pair-density functional the-

ory for iron porphyrin with CAS, RAS, and DMRG active spaces. *The Journal of Physical Chemistry A* **2019**, *123*, 3389–3394.

(72) Derrick, J. S.; Loipersberger, M.; Chatterjee, R.; Iovan, D. A.; Smith, P. T.; Chakarawet, K.; Yano, J.; Long, J. R.; Head-Gordon, M.; Chang, C. J. Metal–Ligand Cooperativity via Exchange Coupling Promotes Iron-Catalyzed Electrochemical CO2 Reduction at Low Overpotentials. *Journal of the American Chemical Society* **2020**, *142*, 20489–20501.

(73) Smith, J. E.; Lee, J.; Sharma, S. Nuclear Gradients of Near-Exact Complete Active Space Self-Consistent Field Wave Functions. *arXiv preprint arXiv:2201.06514* **2022**,

(74) Ortuño, M. A.; Cramer, C. J. Multireference electronic structures of Fe–pyridine (diimine) complexes over multiple oxidation states. *The Journal of Physical Chemistry A* **2017**, *121*, 5932–5939.

(75) Stieber, S. C. E.; Milsmann, C.; Hoyt, J. M.; Turner, Z. R.; Finkelstein, K. D.; Wieghardt, K.; DeBeer, S.; Chirik, P. J. Bis (imino) pyridine iron dinitrogen compounds revisited: differences in electronic structure between four-and five-coordinate derivatives. *Inorganic Chemistry* **2012**, *51*, 3770–3785.

(76) Peverati, R.; Head-Gordon, M. Orbital optimized double-hybrid density functionals. *The Journal of chemical physics* **2013**, *139*, 024110.

(77) Santra, G.; Martin, J. M. Do Double-Hybrid Functionals Benefit from Regularization in the PT2 Term? Observations from an Extensive Benchmark. *The journal of physical chemistry letters* **2022**, *13*, 3499–3506.